

Modelling and optimisation of sound absorption in replicated microcellular metals

Otaru, A.J.^a, Morvan, H.P.^a, Kennedy, A.R.^{b*}

^aGas Turbine & Transmissions Research Centre, Faculty of Engineering, University of Nottingham, NG7 2RD, UK

^{b*} Engineering Department, Lancaster University, Lancaster, LA1 4YW

(a.kennedy3@lancaster.ac.uk)

Abstract

Wilson's poroacoustic model has been shown to be an accurate predictor of sound absorption in porous metals with bottleneck type structures. When used to optimise pore structures, using porosity and permeability as variables, the most broadband absorption is predicted for the highest porosity achievable (approximately 70%) and for a permeability of the order 10^{-10} m². Although performance close to that for glass wool is not possible, with these porosities, specific strength and stiffness exceeding those for many polymers is obtained, making these materials viable for load bearing components with credible soundproofing.

Keywords:

Porous material; simulation; modelling, acoustic, permeability

Noise reduction is of importance for both safety and comfort, across a wide range of industries and is often tackled by using porous in-fill layers of materials, such as foams or wadding, to dissipate sound energy. Open celled metal foams (or more correctly, porous metals) are capable of absorbing sound, but also offer multi-functional performance (e.g. high specific stiffness, good energy absorption and fire resistance) in a self-supporting 3-dimensional form. This uniqueness makes porous metals suitable for a wide range of applications for noise control, where they are candidates to replace complex multi-component structures.

Figure 1 compares the normal incidence absorption coefficient (the fraction of energy from the sound wave that is absorbed when it is incident normal to the surface of a material) for

bottleneck [1] and sponge-type [2] porous metals and compares this with non-structural glass wool (GWF [3]) and sintered metal fibre (SMF [4]) materials. Although this property is dependent upon thickness, and the samples presented range in thickness from roughly 17-25 mm, the figure shows that sound absorption in porous metal structures does not compare favourably with those for established soundproofing materials. Of those presented, absorption is best in porous metals with medium levels of porosity (60-65%) that have so-called “bottleneck” structures, where pores are connected to their neighbours via narrow pore openings or “windows” [1]. The typical structure of such a porous material (also from [1]) is shown in Figure 1. These materials, made by the creation of porosity through pressure-assisted infiltration of a packed bed of a sacrificial “space holder” or “porogen” such as salt, have well-documented relationships between pore and window size and the number of windows per pore [5]. Good sound absorption in these types of structures is attributed to effective energy dissipation via friction with the pore surface, as the air increases in velocity when it travels from the large pores through the much smaller pore openings [6]. With lower porosities than typical porous metals, these porous materials have credible structural performance, particularly if “hard-backed” with an Al sheet on the external surface.

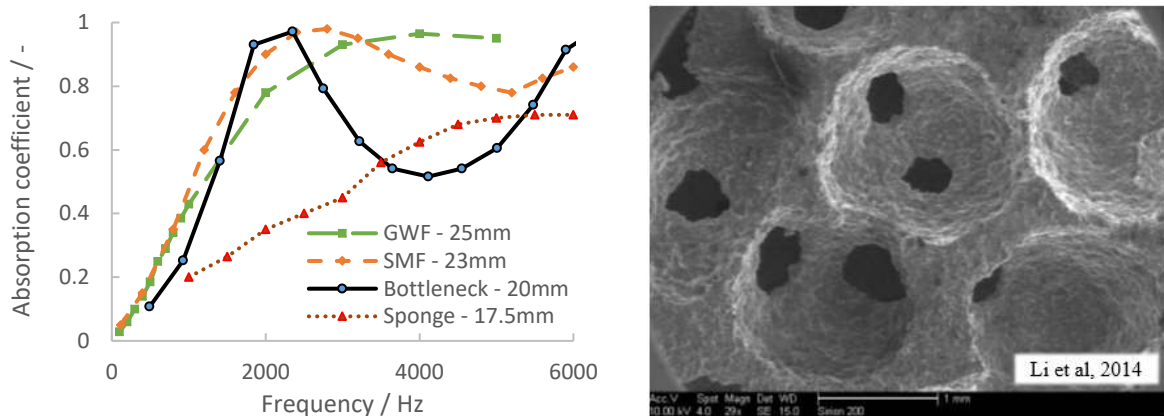


Figure 1 Plots (left) of normal incidence absorption coefficient (A_c) against frequency for hard-backed porous materials [1-4] and (right) an example of porous Al with a bottleneck type structure [1].

The potential to narrow the performance gap between current soundproofing materials and novel, self-supporting sound absorbing structures can be determined through optimisation of the structure of the porous body and its geometry. With numerous combinations of porosity, pore size, window size and absorber thickness being possible, a simulation-based approach

provides the most convenient route to determining the capacity for these materials to absorb sound.

Whilst modelling of sound absorption in more traditional porous structures, and even porous metals, is commonplace, there has been rather limited effort to model sound absorption in bottleneck type structures. It is generally considered, though seldom demonstrated, that established models, such as those by Delaney–Bazley [7], Johnson, Champoux and Allard [8] and Wilson [9] are inappropriate for these types of structures, since these models mostly deal with porous materials where the pores do not abruptly change in cross section. In response to this, Lu et al [10], developed an analytical model to describe sound absorption in semi-open cellular (bottleneck) structures, finding (as did [6,11,12] who compared this model to their experimental measurements for sound absorption in porous metals with bottleneck structures) reasonably good agreement between predictions and experimental measurements, especially at lower frequencies. This model was then used to study the individual effects of porosity, pore size and window size, finding absorption behaviour improving initially as the pore size and window size were decreased (with little influence of porosity), but that with further decreases, the foam became a poorer absorber [10].

Software such as Comsol Multiphysics 5.2™, enables the extension of simple sound absorption modelling to complex 3D structures and non-incident sound wave scenarios, yielding accurate absorption predictions for conventional soundproofing materials. The empirical poroacoustic models of Delany-Bazley-Mikki (DBM), Johnson-Champoux-Allard (JCA) and Wilson (W) are embedded within this software. Despite their questioned applicability for bottleneck structures, they are convenient to use. In addition to inputs for the properties of the fluid, values for parameters such as the permeability, tortuosity, thermal and viscous length are required, which can be determined from directly measurable structural parameters such as the porosity, pore size and window size (for greater detail of the context of these parameters refer to [13]).

Figure 2 plots simulations for sound absorption coefficient against frequency, using a model of a 20 mm thick, hard-backed porous structure within a two-dimensional representation of a standing wave tube (the 2D solution varying insignificantly from the 3D) for key poroacoustic models within Comsol Multiphysics 5.2™ software. Simulations were performed using only the data given in [1,6,10] for porosity, pore size and window size, in combination with well-established expressions for permeability in the Darcy regime [14,15], tortuosity [16], (given in

equations 1 and 2) and thermal and viscous length [17] for porous materials with bottleneck type structures. The permeability for bottleneck structures was developed from models in [14, 15] by expanding the coordination number, N_c , in terms of key structural parameters (shown in equation 2). This was performed by fitting N_c to measurements and modelling in [5], and fitting the permeability through correlation with CFD simulations presented in [18], for the case where the ratio of the window to pore size is in the range of 0.15 to 0.4. The viscous and thermal lengths were approximated to half the window diameter and half the pore diameter respectively [17].

$$\tau = 2 + 2 \cos \left[\frac{4\pi}{3} + \frac{1}{3} \cos^{-1}(2\phi - 1) \right] \quad 1$$

$$k_0 = \frac{1.03 N_c \phi r_w^3}{6\pi r_p} \quad \text{where } N_c = 17 \phi \left(\frac{r_w}{r_p} \right)^{0.27} \quad 2$$

It can be seen that both the DBM (best suited to fibre structures such as glass wool) and the JCA model fail to describe the sound absorption accurately over any portion of the frequency range for the data in [1]. Despite the reported shortcomings, the Wilson model predicts the sound absorption response very accurately for both this sample, those in [1,6] for different pore and window sizes and for samples with different morphologies in [10] (also shown in Figure 2), matching more closely than the model presented therein. The reason for this close fitting is not discussed in detail in this brief paper, but similarities in the model developed and the Wilson model are noted in [10] for structures and frequencies explored in this study.

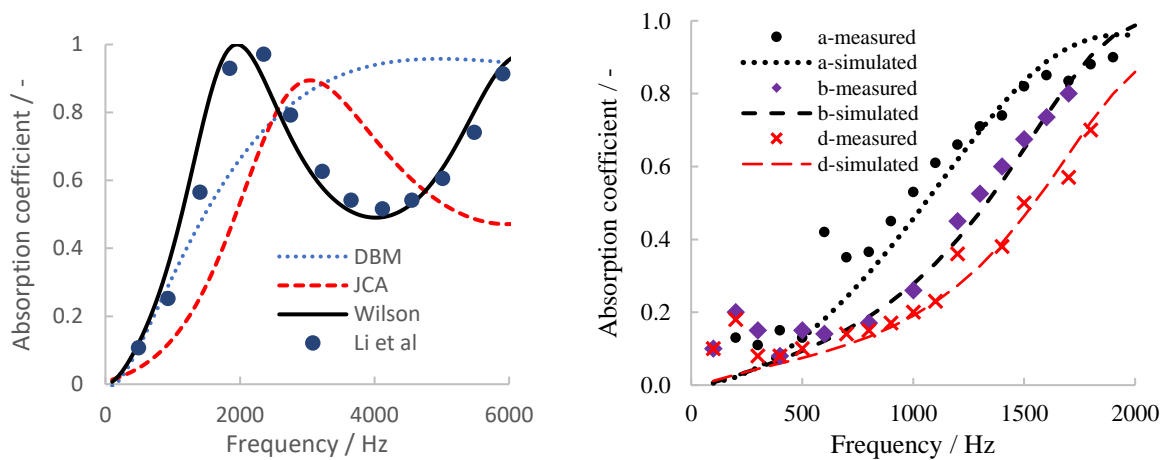


Figure 2. Plots of measured and modelled normal incidence absorption coefficient against frequency for hard-backed 20 mm thick structures (left) for [1] compared with several models and (right) for [10] compared with the Wilson model [9].

With confidence in the Wilson model, optimisation of the acoustic response, to achieve performance more like glass wool, was performed, within the realistic constraints of the materials being modelled and the applicability of the structural models being used. Simulation using the Wilson model only requires specification of the porosity and the permeability to determine the structural parameters needed. Since these porous structures (and the models to describe the permeability) are derived from packed beds of spherical beads, realistic lower and upper limits to the porosity are 0.55 and 0.68 [5]. The realistic permeability range (considering the range in porosity, pore and window size) is much broader, from approximately 10^{-12} to 10^{-7} m².

Figure 3 shows results for 30+ simulations, plotting the noise reduction coefficient (NRC, the arithmetic mean of the sound absorption coefficient at frequencies of 250, 500, 1000 and 2000 Hz) and the peak absorption coefficient ($A_{c \max}$) for a comprehensive array of combinations of permeability, for 20 mm thick samples, across the whole interval of porosities. $A_{c \max}$ and NRC values derived from experimental data from [1,6] are also plotted (as triangles) which overlie the simulation data. Whilst not all the data fall on single curves for each property, there are clear maxima, indicating improved sound absorption in the permeability range of approximately 10^{-10} to 10^{-9} m². It is interesting to note that the experimental data from [1, 6] lie close to the maxima and the best performing samples in [1] and [10] have permeabilities (as calculated using Eq 2) of 5.1×10^{-10} and 4.1×10^{-10} m² respectively. Maxima occur since if the permeability is too high, the velocity of air flow will change little when passing through the pores and the resulting energy dissipation from friction will be low. If the permeability is too low, most of the sound waves will be reflected from the specimen surface, also leading to poor sound absorption [6]. Figure 3 also presents a more focussed study of the effect of the sample thickness on $A_{c \max}$, for samples with the same pore fraction (0.68). As might be expected, decreasing the sample thickness shifts the maxima to slightly lower permeability. For permeability in the range of approximately 7 to 9×10^{-10} m², $A_{c \max}$ is close to unity over the entire thickness range (10 - 40 mm). For higher permeability, peak absorptions increase as the

thickness increases, the reverse is true for lower permeability. This insight helps clarify the variable dependence upon thickness observed in the literature, in particular in [19].

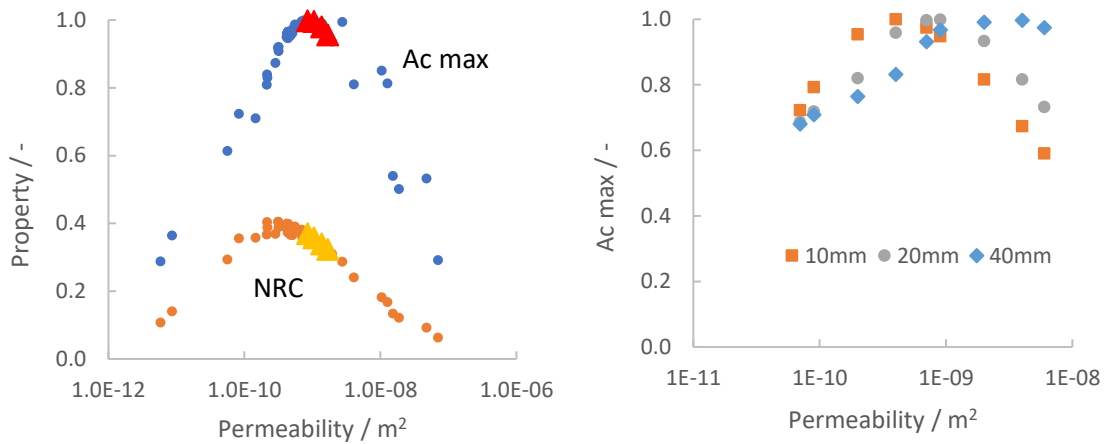


Figure 3. Plots of sound absorption behaviour against permeability for (left) 20 mm thick samples with a range of porosities and (right) for samples with different thickness and a constant porosity (0.68).

Neither the NRC nor Ac max values describe the absorption response across the whole range of frequencies of interest. More complete optimisation requires minimising the characteristic dip in absorption in the mid-range of frequencies, as was evident for the bottleneck structure in Figure 1. Figure 4 plots the effect of pore fraction, for a 20 mm thick sample with the highest NRC value (with a permeability of $4 \times 10^{-10} \text{ m}^2$), showing that the highest porosity gives the highest peak, shifting it to slightly higher frequency, and the lowest dip (an effect which is similar to that observed in [6], but more pronounced than in the model in [10]). For this maximum pore fraction (0.68), a wide range of permeability is plotted, showing that despite it being possible to increase the peak absorption by increasing the permeability from $4 \times 10^{-10} \text{ m}^2$ to $7 \times 10^{-10} \text{ m}^2$ (as was evident in Figure 3), this comes with the penalty of a greatly increased dip in absorption at frequencies close to 4000 Hz. Specific applications will drive the balance between the need for maximum or more broadband absorption behaviour and the final choice that is made, but the maxima in Ac max and NRC appear to bound the optimum search area.

To achieve the target permeability, for a given pore size and fraction, equation 2 can be rearranged to define the target window size, which can be achieved by varying the pressure difference used to affect infiltration [5]. Unlike as suggested by [10], this process suggests there is not a unique optimum pore opening size or optimum ratio of pore to opening diameter.

In the context of other studies with pore diameters in the range of 0.5 - 2.0 mm, the target ratio varies from roughly 0.3 to 0.1, consistent with suggested “optimum” pore openings of the order of 0.1 mm [10,20].

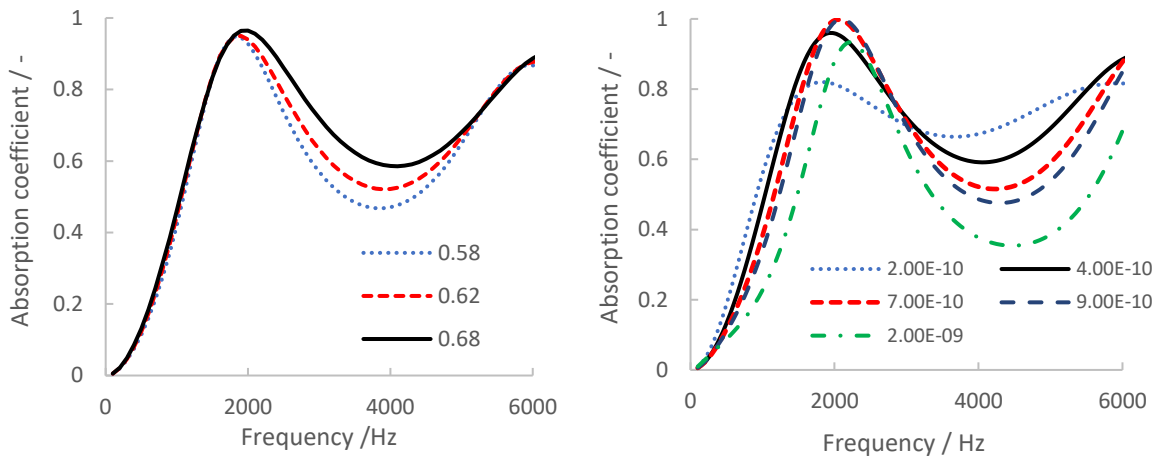


Figure 4 Plots of modelled normal incidence absorption coefficient against frequency for 20 mm thick structures (a) as a function of pore fraction and constant permeability ($4 \times 10^{-10} \text{ m}^2$) and (b) as a function of permeability and constant pore fraction (0.68).

The Wilson model has been seen to be reliable for simulating sound absorption in porous metals with bottleneck structures and can be used as a tool to optimise porous structures using their porosity and permeability as variables. Optimisation predicts that it is possible to increase peak absorption and reduce the dip, compared with the performance of the bottleneck type porous metal presented in [1] in Figure 1, by decreasing the permeability. Optimum permeability is, however a (weak) function of sample thickness. Despite modelling indicating higher porosity is favourable (and indeed that further improved broadband absorption would be realised if the porosity could be increased further), achieving soundproofing performance close to that for glass wool is not possible. However, with porosities of 68%, strengths and densities similar to those for many polymers is achieved in these materials [21] with a stiffness which (even without a backing material) is at least twice that for most polymers, making these materials viable for load bearing components with credible soundproofing.

Acknowledgments

OAJ would like to acknowledge funding from the Dean’s Award made by the University of Nottingham.

References

1. Y. Li, L. Zhendong, F. Han, *Procedia Materials Science*, 4 (2014) 187-190.
2. B. Hinze, J. Rösler, *Advanced Engineering Materials*, 16 (2014) 284–288.
3. N. Kino, T Ueno, *J. App. Acoustics*, 69 (2008) 325-331.
4. Z. Bo, C. Tianning, *Applied Acoustics*, 70 (2009) 337-346.
5. P. Langston, A.R. Kennedy, *Powder Technology*, 268 (2014) 210-218.
6. Y. Li, X. Wang, X. Wang, Y. Ren, F. Han, C. Wen, *Journal of Applied Physics*, 110, (2011) 113525.
7. M. E. Delany, E. N. Bazley, *Appl. Acoust.*, 3 (1969) 105-116.
8. J. F. Allard, Y. Champoux, *J. Acoust. Soc. Am.*, 91 (1992) 3346-3353.
9. D. K. Wilson, *J. Acoust. Soc. Am.*, 94 (1993) 1136-1145.
10. T.J. Lu, F. Chen, D. He, *J. Acoust. Soc. Am.*, 108 (2000) 1697-1708.
11. M Hakamada, T Kuromura, Y Chen, H Kusuda, M Mabuchi, *Applied Physics Letts.*, 88 (2006) 254106.
12. M Hakamada, T Kuromura, Y Chen, H Kusuda, M Mabuchi, *J. Applied Physics*, 100 (2006) 114908.
13. <http://apmr.matelys.com/index.html> (accessed 21/02/2018)
14. J. Despois, A Mortensen, *Acta Materialia* 53 (2005) 1381-1388.
15. E.L. Furman, A.B. Finkelstein, M.L. Cherny, *Metals*, 3 (2013) 49-57.
16. G. J. F. Smit, J. P. Du Plessis, *Chemical Engineering Science*, 54 (1999) 645-654.
17. R Panneton, X Olny, *J. Acoust. Soc. Am.*, 119 (2006) 2027.
18. A.J. Otaru, A.R. Kennedy, *Scripta Materialia*, 124 (2016) 30-33.
19. F. Han, G. Seiffert, Y. Zhao, B. Gibbs, *J. Phys. D: Appl. Phys.* 36 (2003) 294-302.
20. X. W. Wang, T. J. Lu, *J. Acoust. Soc. Am.*, 106, (1999) 756-765.
21. A Wright, A R Kennedy, *Adv. Eng. Mater* 19 (2017) 1600467.